Nonthermal direct photons in Pb+Pb at 160*A* GeV from microscopic transport theory

A. Dumitru, M. Bleicher, S. A. Bass, C. Spieles, L. Neise, H. Stöcker, and W. Greiner
Institut für Theoretische Physik der J.W. Goethe-Universität, Postfach 111932, D-60054 Frankfurt a.M., Germany
(Received 30 September 1997)

Direct photon production in central Pb+Pb collisions at CERN-SPS energy is calculated within the ultrarelativistic quantum molecular dynamics model (UrQMD), and within distinctly different versions of relativistic hydrodynamics. We find that in UrQMD the local momentum distributions of the secondaries are strongly elongated along the beam axis initially. Therefore, the pre-equilibrium contribution dominates the photon spectrum at transverse momenta above ≈1.5 GeV. The hydrodynamics prediction of a strong correlation between the temperature and radial expansion velocities on the one hand, and the slope of the transverse momentum distribution of direct photons on the other hand thus is not recovered in UrQMD. The rapidity distribution of direct photons in UrQMD reveals that the initial conditions for the longitudinal expansion of the photon source (the meson ''fluid'') resemble boost invariance rather than Landau-like flow.
[S0556-2813(98)00706-7]

PACS number(s): 25.75.Dw, 12.38.Mh, 24.10.Lx, 24.85.+p

The radiation of real and virtual photons has frequently been proposed as a diagnostic tool for the hot and dense matter created in (ultra)relativistic heavy-ion collisions [1,2]. The mean free path of photons with high transverse momentum exceeds the expected source sizes by one order of magnitude [2,3]. Hard photons thus can give insight into the early stage of these reactions.

Transverse momentum-dependent upper limits for direct photon production in central S+Au collisions at 200*A* GeV have been published by the WA80 Collaboration [4] (see also the data of the CERES Collaboration [5]). These data initiated theoretical studies [6–9] which showed that direct photon production is strongly overestimated if the photon source is thermalized (having an initial energy density of $2-5$ GeV/fm^3) and if one assumes that it is composed of light mesons only (say π, η, ρ, ω). Due to the low specific entropy of these particles a reasonable final-state multiplicity of secondaries and a maximum temperature that is consistent with the WA80 data ($T_{\max}\leqslant 300$ MeV) cannot be achieved simultaneously (at least if the expansion is approximately isentropic).

Most of the calculations quoted (except those of Ref. [7]), however, assumed that the photon source is in local thermal equilibrium and that ideal hydrodynamics can be applied to determine the space-time evolution of the temperature. Here, we perform a calculation within the microscopic transport model UrQMD, which includes the pre-equilibrium contributions to direct photon production. This is of particular relevance in view of the fact that local thermalization (i.e., locally isotropic momentum distributions) in (ultra)relativistic heavy-ion collisions is probably not achieved within the first few fm/c [10,11] where the high-k_T photons are produced. Since neither thermal nor chemical equilibrium is assumed, the effects of finite viscosity (i.e., finite mean free paths) [12] and inhomogeneous or fluctuating energy density distributions [13] are included. Comparisons of the transverse momentum and rapidity distributions of direct photons with those calculated within two fluid-dynamical models are made.

The calculations presented here are based on the UrQMD model [14], which spans the entire presently available range of energies from GSI-SIS to CERN-SPS. Its collision term contains 50 different baryon species (including nucleon, delta, and hyperon resonances with masses up to 2.2 GeV) and 25 different meson species (including strange meson resonances), which are supplemented by their corresponding antiparticles and all isospin-projected states.

The model is based on the covariant propagation of all hadrons on classical trajectories, excitation of resonances and strings and their subsequent decay, respectively, fragmentation. UrQMD accounts for secondary interactions: the annihilation of produced mesons on baryons can lead to the formation of s-channel resonances or strings. Free cross sections for hadron-hadron scattering in the hot and dense nuclear matter are employed. Comparisons of UrQMD calculations to experimental hadron yields from SIS to SPS are documented elsewhere [14].

We briefly discuss the two most important reactions for the creation of direct photons. Below 2 GeV center of mass energy intermediate resonance states are excited. The total cross section for these reactions are given by

$$\sigma_{\rm tot}^{M_1M_2}(\sqrt{s})=\sum_{R=\rho,f_2,\ldots}\langle j_{M_1},m_{M_1},j_{M_2},m_{M_2}\|J_R,M_R\rangle \times\frac{2I_R+1}{(2I_{M_1}+1)(2I_{M_2}+1)} \times\frac{\pi}{p_{\rm c.m.}^2}\frac{\Gamma_{R\to M_1M_2}\Gamma_{\rm tot}}{(M_R-\sqrt{s})^2+\Gamma_{\rm tot}^2/4}, \qquad (1)$$

which depends on the total decay width $\Gamma_{\rm tot}$, the partial decay width $\Gamma_{R\to M_1M_2}$, and on the c.m. energy $\sqrt{s}$. The corresponding isospins, isospin-projections, and spins are denoted by j, m, I, respectively. At higher energies these processes become less important. One then enters the region of t-channel scattering of the hadrons.

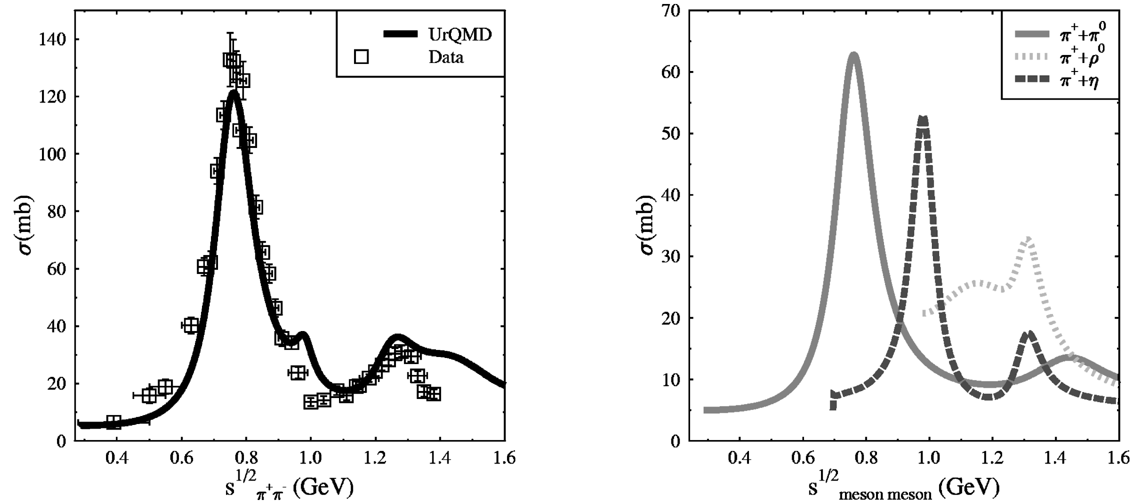

FIG. 1. Total cross sections of $\pi^+\pi^-$ and various other meson-meson reactions as calculated within the UrQMD model, data from Ref. [15].

In Fig. 1 (left) the total $\pi^+\pi^-$ cross section as calculated within UrQMD is compared to experimental data [15]. Below 1 GeV the cross section is dominated by the ρ resonance, while at higher energy the $f_2(1270)$ is more important.

Figure 2 shows the distribution of $\pi\pi$ collisions with a given relative rapidity in a given spacial direction (upper indices refer to the particle number):

$$\Delta y_{x,y,z} = \frac{1}{2}\ln\frac{E^1 + p^1_{x,y,z}}{E^1 - p^1_{x,y,z}} - \frac{1}{2}\ln\frac{E^2 + p^2_{x,y,z}}{E^2 - p^2_{x,y,z}}. \quad (2)$$

One observes that most collisions occur at $|\Delta y| < 3$. In this range the collision spectrum is nearly isotropic. In the longitudinal direction, however, there is an additional component above $|\Delta y_z| = 3$. This is due to pions created in the fragmentation of a color flux tube close to projectile and target rapidities. In $p(200A\ \text{GeV}) + p$ collisions $\approx 15\%$ of all pions have $|y^{\pi}_{\text{c.m.}}| > 2$ [16]. Note that not all of these collisions are forbidden by the finite formation time of secondaries since the fragmentation region mesons contain one of the initial valence quarks (i.e., the sources of the color field). Thus, even within the formation time, these mesons may interact with half of the free meson cross section in the UrQMD model. Obviously, these meson-meson collisions with large longitudinal rapidity difference are not taken into account in hydrodynamical calculations. However, as will be discussed below, it is just their contribution which dominates the direct photon spectrum above $k_T \approx 1.5$ GeV.

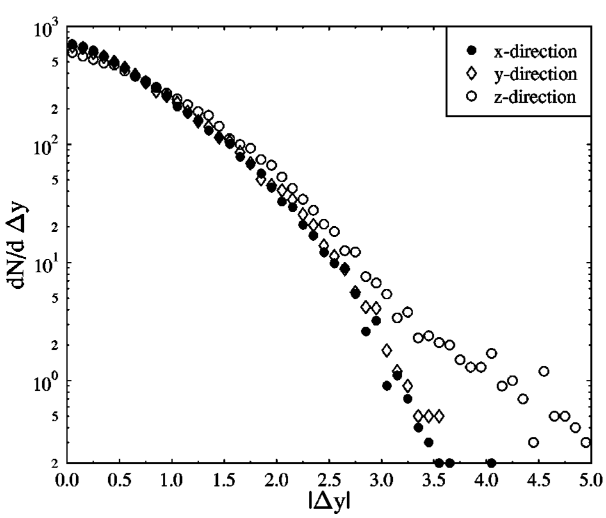

FIG. 2. Number of $\pi\pi$ collisions as a function of the rapidity difference in the three spacial directions (Pb+Pb, $E_{\text{lab}} = 160A$ GeV, $b = 0$ fm).

Let us now get to the reference equilibrium calculations of direct photon production within hydrodynamics. In the first model, we assume a three-dimensional expansion with cylindrical symmetry and longitudinal boost invariance [17]. Here, the dynamical creation of the fluid of secondaries in space-time is ignored and only the expansion stage is treated. The initial temperature and time are taken as 300 MeV and $\tau_0 = 0.22$ fm/c, respectively.

In the three-fluid model, fluids 1 and 2 correspond to projectile and target, while fluid 3 represents the newly produced particles around midrapidity. Fluids 1 and 2 are coupled via source terms leading to energy and momentum exchange. These interactions are due to binary collisions of the nucleons in the respective fluids and are derived from nucleon-nucleon data. A detailed discussion of this model as well as results (pion rapidity and transverse momentum spectra at CERN-SPS, baryon stopping and directed flow at AGS and SPS, the width of the compression shock waves, etc.) can be found in Refs. [9,18,19].

In the hydrodynamical calculations the fluid of produced particles is assumed to be the hottest, and thus the dominant source of high-k_T photons. It's equation of state is that of an ideal gas of massive π, η, ρ, and ω mesons below $T_C = 160$ MeV. For $T > T_C$ we assume an ideal quark-gluon plasma (QGP) (massless, noninteracting u, d quarks and gluons) described within the MIT bag-model [20]. The bag constant is chosen such that the pressures of the two phases match at $T = T_C$ ($B^{1/4} = 235$ MeV) thus leading to a first order phase transition.

The number of emitted direct photons in each of the three phases is parametrized as [2]

$$E\frac{dN^{\gamma}}{d^4x\ d^3k}=\frac{5\alpha\alpha_S}{18\pi^2}T^2e^{-E/T}\ln\left(\frac{2.912E}{g^2T}+1\right). \qquad (3)$$

E is the photon energy in the local rest frame. In our calculations we fix $\alpha_S=g^2/4\pi=0.4$. Equation (3) accounts for pion annihilation ($\pi\pi\rightarrow\rho\gamma$), and Compton-like scattering ($\pi\rho\rightarrow\pi\gamma$, $\pi\eta\rightarrow\pi\gamma$) off a ρ or η meson (in lowest order perturbation theory). In the QGP phase, alternatively, quark-antiquark annihilation ($q\overline{q}\rightarrow g\gamma$) and Compton-like scattering of a quark or antiquark off a gluon ($q,\overline{q}+g\rightarrow q,\overline{q}+\gamma$) are considered. Contributions from the A_1 meson [21], as well as the effect of hadronic formfactors [2], are neglected since they are of the same magnitude as higher order corrections to Eq. (3), which we have also not taken into account. Also, the number of processes that contribute to direct photon production enhances the rate only linearly, while the temperature distribution enters exponentially. Our main interest here is not the absolute photon yield but rather the effective temperature of the direct photons, i.e., the inverse slope of their transverse momentum spectrum.

The photon spectrum emitted in a heavy-ion collision is obtained here by an (incoherent) integration over space-time:

$$\frac{dN^{\gamma}}{d^2k_T\ dy}=\int d^4x\ E\frac{dN^{\gamma}}{d^4x\ d^3k}. \qquad (4)$$

To allow for a comparison with the hydrodynamical calculations we have considered the same processes also in the UrQMD model, namely, $\pi^{\pm}\pi^{\mp}\rightarrow\rho^0\gamma$, $\pi^{\pm}\pi^0\rightarrow\rho^{\pm}\gamma$, $\pi^{\pm}\rho^0\rightarrow\pi^{\pm}\gamma$, $\pi^{\pm}\rho^{\mp}\rightarrow\pi^0\gamma$, $\pi^0\rho^{\pm}\rightarrow\pi^{\pm}\gamma$, $\pi^{\pm}\eta\rightarrow\pi^{\pm}\gamma$. Of course, in UrQMD these processes are considered explicitly (we employ the differential cross sections given in Ref. [2]) and are not folded with thermal distribution functions, nor with a thermal $\sqrt{s}$ distribution of meson-meson collisions. We find that the $\pi\rho\rightarrow\pi\gamma$ and $\omega\rightarrow\pi\gamma$ processes are dominant in the range $1\leqslant k_T\leqslant 3$ GeV. This is due to the fact that, in addition to the kinetic energy, also the mass of the ρ or ω can be converted into photon energy. In contrast to the thermal rate (3), in the UrQMD model m_ρ and m_ω are smeared out according to a Breit-Wigner distribution. For the processes $\pi\pi\rightarrow\rho\gamma$ we have, however, assumed that the ρ meson in the final state is produced with the peak mass of 770 MeV. Since free current quarks and gluons have not been included in the present version of the UrQMD model, the processes $q\overline{q}\rightarrow g\gamma$, etc., are not considered there.

The various transverse momentum distributions of direct photons, see Fig. 3, reflect the distinct cooling laws within the two fluid-dynamical models. The faster the cooling of the photon source, the steeper the slope of the photon spectrum. An exponential fit of the spectrum in the region $2\leqslant k_T\leqslant 3$ GeV yields $T=260$ MeV for the three-fluid model, and $T=210$ MeV for the Bjorken expansion.

If we take into account only the ''thermal'' meson-meson collisions with rapidity gap $|\Delta y_z|<3$, we find a similar photon spectrum in the UrQMD model as in scaling hydrodynamics. The fact that the hadronic mass spectrum in UrQMD has no upper limit leads to a collision spectrum of the light mesons that is as ''cool'' as in the hydrodynamic calculations, if there a first order phase transition at a critical temperature around 160 MeV is assumed (see also Ref. [8]). In UrQMD, a significant part of the energy density can be stored into heavy meson and baryon resonances. This keeps the pressure[1] and temperature low [10,22]. We have analyzed the temperature as a function of energy density (at normal nuclear matter baryon density) in UrQMD in Ref. [14].

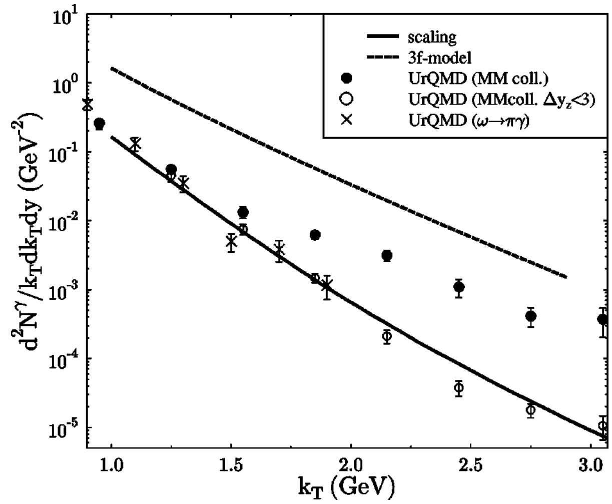

FIG. 3. Transverse momentum spectrum of direct photons at midrapidity (Pb+Pb, $E_{\rm lab}=160A$ GeV, $b=0$ fm). The lines refer to hydrodynamical calculations including a first order phase transition to a QGP at $T_C=160$ MeV [three-fluid model (dashed), and scaling expansion (solid)]. The result of the UrQMD calculation with all meson-meson collisions (full circles) is compared to the calculation with only ''thermal'' meson-meson collisions (open circles). Crosses show the photons from ω-meson decays, which are as many as those from ''thermal'' meson-meson collisions. Above $k_T\approx1.5$ GeV the pre-equilibrium contribution dominates.

One also observes that the ''pre-equilibrium'' meson-meson collisions with $|\Delta y_z|>3$ dominate the emission of direct photons with large transverse momenta, $k_T>1.5$ GeV. Obviously, this contribution has nothing to do with high meson transverse momenta (''temperatures'') or fast collective radial expansion. It is thus not included in the hydrodynamic calculations. Hence, the strong correlation between the (Doppler-shifted) temperature and the slope of the photon transverse momentum distribution predicted by the hydrodynamical calculations (see also Refs. [6,8,9,23]) is not seen in UrQMD. Meson-baryon and baryon-baryon processes may further enhance the pre-equilibrium contribution [24]. Below $k_T=1.5$ GeV the photons are dominantly produced by ''thermal'' meson-meson collisions and $\omega\rightarrow\pi\gamma$ decays.

The rapidity distribution of the secondaries (or, alternatively, of the temperature) at early times is very different in the various hydrodynamical models [18,25]. While $T(\eta)$ (η denotes the fluid rapidity) is strongly peaked around midrapidity in the three-fluid model, scaling flow $v_z=z/t$ and energy-momentum conservation $\partial_\mu T^{\mu\nu}=0$ imply that the pressure $p(T,\mu_B)$ is independent of the fluid rapidity $\partial_\eta p$

[1] In future work it has to be checked, however, if UrQMD generates sufficient radial flow to reproduce the measured transverse momentum distributions of mesons.

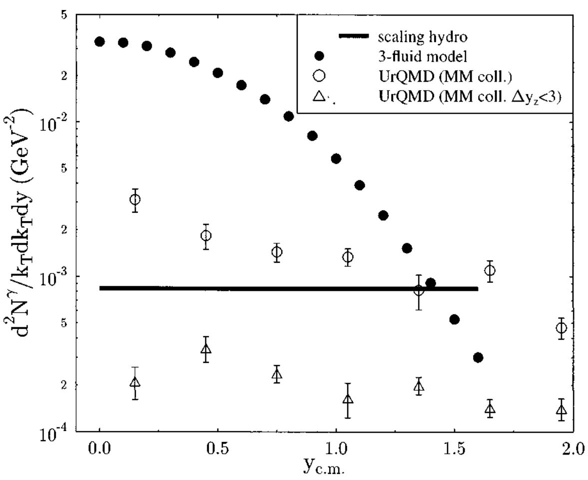

FIG. 4. Rapidity distribution of direct photons, calculated within the various hydrodynamical models (for $k_T=2$ GeV) and UrQMD (for $k_T=2.15$ GeV).

$=0$ and depends only on proper time $\tau=\sqrt{t^2-z^2}$. For net baryon-free matter $\partial_\eta T=0$ follows. However, even in the first case matter is accelerated by a (longitudinal) rarefaction wave, leading to a broadening of the rapidity distribution. Thus, in any case, at the late freeze-out stage the rapidity distribution of secondaries (around midrapidity) will be more or less flat. On the other hand, the rapidity distribution of direct photons with transverse momenta much larger than the maximum temperature of the photon source (e.g., $k_T\approx 2$ GeV at SPS) offers the opportunity to measure the rapidity distribution of the hot photon source *at early times* [25]. This is demonstrated in Fig. 4. In the three-fluid model the photon rapidity distribution is strongly peaked around midrapidity. It is not proportional to the (squared) rapidity distribution of the pions, which are emitted at a much later freeze-out stage. The distribution obtained within UrQMD only resembles that for a boostinvariant expansion, if only ''thermal'' meson-meson collisions are taken into account. The full calculation, however, predicts a maximum of the photon-dN/dy at midrapidity. Nevertheless, the photon distribution is considerably flatter than in the three-fluid model, which shows a concave curvature in this logarithmic plot. This is a consequence of the longitudinal velocity profile [26] induced by the (longitudinal) rarefaction wave accelerating the fluid that is initially at rest. The UrQMD calculation does not exhibit this characteristic feature.

In summary, we have calculated direct photon production in central Pb+Pb collisions at CERN-SPS energy within a microscopic transport model (UrQMD). Within this model, secondary hadron production is described by color flux tube fragmentation and resonance decay. This leads to nonthermal momentum distributions, i.e., they are strongly elongated along the beam axis initially. The contribution from this pre-equilibrium stage to direct photon production is found to dominate at transverse momenta above ≈ 1.5 GeV. Thus, within the UrQMD model, the slope of the photon transverse momentum spectrum is not directly related to the Doppler-shifted ''transverse temperature'' of the source, as it is in hydrodynamics.

If only ''thermal'' meson-meson collisions are taken into account, both the transverse momentum and rapidity spectra of direct photons in UrQMD resemble those calculated within boostinvariant hydrodynamics, if for the latter one assumes an initial temperature $T_i=300$ MeV and initial time $\tau_i=0.22$ fm. This is so although QGP formation is not assumed in UrQMD. Hence, heavy resonances and color flux tubes allow for a rather soft meson-meson collision spectrum even at high entropies.

This work was supported by Graduiertenkolleg Theoretische und Experimentelle Schwerionenphysik, BMBF, DFG, and GSI. M. Bleicher thanks the Josef Buchmann foundation for financial support.

[1] See, e.g., E.V. Shuryak, Phys. Lett. **78B**, 150 (1978); B. Sinha, *ibid.* **128B**, 91 (1983); L. McLerran and T. Toimela, Phys. Rev. D **31**, 545 (1985); P.V. Ruuskanen, Nucl. Phys. **A544**, 169c (1992): J. Kapusta, *ibid.* **A566**, 45c (1994); B. Müller, Rep. Prog. Phys. **58**, 611 (1985); J.W. Harris and B. Müller, Annu. Rev. Nucl. Part. Sci. **46**, 71 (1996).
[2] J. Kapusta, P. Lichard, and D. Seibert, Phys. Rev. D **44**, 2774 (1991).
[3] M.H. Thoma, Phys. Rev. D **51**, 862 (1995).
[4] R. Albrecht *et al.*, Phys. Rev. Lett. **76**, 3506 (1996).
[5] R. Baur *et al.*, Z. Phys. C **71**, 571 (1996).
[6] D.K. Srivastava and B. Sinha, Phys. Rev. Lett. **73**, 2421 (1994); N. Arbex, U. Ornik, M. Plümer, A. Timmermann, and R.M. Weiner, Phys. Lett. B **345**, 307 (1995); J.J. Neumann, D. Seibert, and G. Fai, Phys. Rev. C **51**, 1460 (1995): Y. Tarsov, Phys. Lett. B **379**, 279 (1996); C.M. Hung and E.V. Shuryak, Phys. Rev. C **56**, 453 (1997).
[7] E.L. Bratkovskaya and W. Cassing, Nucl. Phys. **A619**, 413 (1997); G.Q. Li, G.E. Brown, and C.M. Ko, nucl-th/9706022; G.Q. Li and G.E. Brown, nucl-th/9706076.
[8] J. Sollfrank, P. Huovinen, M. Kataja, P.V. Ruuskanen, M. Prakash, and R. Venugopalan, Phys. Rev. C **55**, 392 (1997); J. Cleymans, K. Redlich, and D.K. Srivastava, *ibid.* **55**, 1431 (1997).
[9] A. Dumitru, U. Katscher, J.A. Maruhn, H. Stöcker, W. Greiner, and D.H. Rischke, Phys. Rev. C **51**, 2166 (1995).
[10] H. Sorge, Phys. Lett. B **402**, 251 (1997).
[11] R. Mattiello, C. Hartnack, A.v. Keitz, J. Schaffner, H. Sorge, H. Stöcker, and C. Greiner, Nucl. Phys. (Proc. Suppl.) **24B**, 221 (1991).
[12] P. Danielewicz, Phys. Lett. **146B**, 168 (1984); P. Danielewicz and M. Gyulassy, Phys. Rev. D **31**, 53 (1985); A. Hosoya, and K. Kajantie, Nucl. Phys. **B250**, 666 (1985); K. Haglin and S. Pratt, Phys. Lett. B **328**, 255 (1994).
[13] C. Spieles, L. Gerland, H. Stöcker, C. Greiner, C. Kuhn, and J.P. Coffin, Phys. Rev. Lett. **76**, 1776 (1996); M. Gyulassy, D.H. Rischke, and B. Zhang, Nucl. Phys. **A613**, 397 (1997).
[14] M. Bleicher *et al.*, ''Structure of Vacuum and Elementary Matter,'' in *Proceedings of the International Conference on Nuclear Physics at the Turn of the Millenium,* Wilderness/

George, South Africa, 1996 (World Scientific, Singapore, 1997), p. 452; S. Bass *et al.*, *ibid.*, p. 399.

[15] S.D. Protopopescu *et al.*, Phys. Rev. D **7**, 1279 (1973).

[16] T. Kafka *et al.*, Phys. Rev. D **16**, 1261 (1977).

[17] K. Kajantie and L. McLerran, Phys. Lett. **119B**, 203 (1982); Nucl. Phys. **B214**, 261 (1983); J.D. Bjorken, Phys. Rev. D **27**, 140 (1983); K. Kajantie, R. Raitio, and P.V. Ruuskanen, Nucl. Phys. **B222**, 152 (1983); H. von Gersdorff, M. Kataja, L. McLerran, and P.V. Ruuskanen, Phys. Rev. D **34**, 794 (1986).

[18] A. Dumitru, J. Brachmann, M. Bleicher, J.A. Maruhn, H. Stöcker, and W. Greiner, Heavy Ion Phys. **5**, 357 (1997).

[19] J. Brachmann, A. Dumitru, J.A. Maruhn, H. Stöcker, W. Greiner, and D.H. Rischke, Nucl. Phys. **A619**, 391 (1997).

[20] A. Chodos, R.L. Jaffe, K. Johnson, C.B. Thorn, and V.F. Weisskopf, Phys. Rev. D **9**, 3471 (1974); S.A. Chin, Phys. Lett. **78B**, 552 (1978): E.V. Shuryak, Phys. Rep. **61**, 71 (1980); J. Cleymans, R.V. Gavai, and E. Suhonen, *ibid.* **130**, 217 (1986); H. Stöcker and W. Greiner, *ibid.* **137**, 277 (1986).

[21] L. Xiong, E. Shuryak, and G.E. Brown, Phys. Rev. D **46**, 3798 (1992); C. Song, Phys. Rev. C **47**, 2861 (1983).

[22] H. Stöcker, W. Greiner, and W. Scheid, Z. Phys. A **286**, 121 (1978): H. Stöcker, A.A. Ogloblin, and W. Greiner, *ibid.* **303**, 259 (1981): H. Bebie, P. Gerber, J.L. Goity, and H. Leutwyler, Nucl. Phys. **B378**, 95 (1992).

[23] D. Seibert, Z. Phys. C **58**, 307 (1983).

[24] C. Spieles, L. Gerland, N. Hammon, M. Bleicher, S.A. Bass, H. Stöcker, and W. Greiner, hep-ph/9706525.

[25] A. Dumitru, U. Katscher, J.A. Maruhn, H. Stöcker, W. Greiner, and D.H. Rischke, Z. Phys. A **353**, 187 (1995).

[26] D.H. Rischke, S. Bernard, and J.A. Maruhn, Nucl. Phys. **A595**, 346 (1995).